

Journal Pre-proofs

The influence of moisture on the storage stability of co-amorphous systems

Jingwen Liu, Thomas Rades, Holger Grohganz

PII: S0378-5173(21)00607-4

DOI: <https://doi.org/10.1016/j.ijpharm.2021.120802>

Reference: IJP 120802

To appear in: *International Journal of Pharmaceutics*

Received Date: 21 May 2021

Revised Date: 11 June 2021

Accepted Date: 12 June 2021



Please cite this article as: J. Liu, T. Rades, H. Grohganz, The influence of moisture on the storage stability of co-amorphous systems, *International Journal of Pharmaceutics* (2021), doi: <https://doi.org/10.1016/j.ijpharm.2021.120802>

This is a PDF file of an article that has undergone enhancements after acceptance, such as the addition of a cover page and metadata, and formatting for readability, but it is not yet the definitive version of record. This version will undergo additional copyediting, typesetting and review before it is published in its final form, but we are providing this version to give early visibility of the article. Please note that, during the production process, errors may be discovered which could affect the content, and all legal disclaimers that apply to the journal pertain.

© 2021 The Author(s). Published by Elsevier B.V.

The influence of moisture on the storage stability of co-amorphous systems

Jingwen Liu, Thomas Rades* and Holger Grohganz

Jingwen Liu: Formal analysis, Investigation, Visualization, Writing - original draft.

Thomas Rades: Conceptualization, Methodology, Project administration, Writing – review & editing, Supervision

Holger Grohganz: Conceptualization, Methodology, Writing – review & editing, Supervision

Department of Pharmacy, University of Copenhagen, Universitetsparken 2, 2100 Copenhagen,
Denmark

*** Corresponding author**

E-mail: thomas.rades@sund.ku.dk; Telephone: +45 35336032

Abstract

Co-amorphization has been utilized to improve the physical stability of the respective neat amorphous drugs. However, physical stability of co-amorphous systems is mostly investigated under dry conditions, leaving the potential influence of moisture on storage stability unclear. In this study, carvedilol-L-aspartic acid (CAR-ASP) co-amorphous systems at CAR to ASP molar ratios from 3:1 to 1:3 were investigated under non-dry conditions at two temperatures, i.e., 25 °C 55%RH and 40 °C 55%RH. Under these conditions, the highest physical stability of CAR-ASP systems was observed at the 1:1 molar ratio. This finding differed from the optimal molar ratio previously obtained under dry conditions (CAR-ASP 1:1.5). Molecular interactions between CAR and ASP were affected by moisture, and salt disproportionation occurred during storage. Morphological differences of systems at different molar ratios could be observed already after one week of storage. Furthermore, variable temperature X-ray powder diffraction measurements showed that excess CAR or excess ASP, existing in the binary systems, resulted in a faster recrystallization compared to equimolar system. Overall, this study emphasizes the influence of moisture on co-amorphous systems during storage, and provides options to determine the optimal ratio of co-amorphous systems in presence of moisture at comparatively short storage times.

Keywords: co-amorphous; moisture; molar ratio; physical stability; recrystallization

1. Introduction

Aqueous solubility of active pharmaceutical ingredients is a critical drug property that needs to be considered in the development of oral drug delivery formulations since poor aqueous solubility often results in a low and variable oral absorption, and thus a low and variable bioavailability with a potentially limited pharmacological effect (Babu and Nangia, 2011; Savjani et al., 2012). The use of amorphous forms of drug candidates is a promising approach to overcome this poor aqueous solubility challenge (Bikiaris, 2011; Grohganz et al., 2013; Kawabata et al., 2011). Amorphous forms exhibit higher internal energy and reactivity compared with their crystalline counterparts (Hancock and Zografi, 1997). Therefore, a drug in an amorphous form potentially provides an increased dissolution rate and an improved apparent solubility compared with the respective crystalline state(s) (Laitinen et al., 2017). However, the amorphous form is thermodynamically unstable, and as a result tends to undergo spontaneous recrystallization, leading to a risk in formulation development with regard to the drug's physical instability (Korhonen et al., 2017).

Co-amorphization has been developed as a suitable method to stabilize the inherently unstable amorphous form of drugs (Dengale et al., 2016; Laitinen et al., 2013). In co-amorphous systems, two or more, initially crystalline, low-molecular weight components form a homogeneous single-phase amorphous mixture upon processing (Dengale et al., 2016; Liu et al., 2021). Different stabilization mechanisms of co-amorphous systems have been identified, including molecular interactions between the drug and the co-former, intimate molecular-level mixing and an elevated glass transition temperature (T_g) compared to the pure drug (Dengale et al., 2014; Han et al., 2020; Löbmann et al., 2013; Löbmann et al., 2012). Most physical stability tests of co-amorphous systems reported in the scientific literature were conducted at dry conditions, whilst only 18.7% of the totally studied co-amorphous systems also cover physical stability under humid conditions

(Liu et al., 2021). Under humid storage conditions, moisture can be absorbed by the co-amorphous system and influence the various contributors to stabilization by disturbing molecular interactions, reducing the T_g , increasing molecular mobility and promoting amorphous-amorphous phase separation and recrystallization (Andronis et al., 1997; Jensen et al., 2016; Rumondor and Taylor, 2010). In addition, the optimal molar ratio to achieve the highest physical stability in co-amorphous systems closely links to these stabilization contributors, thus it is reasonable to assume that the optimal molar ratio to achieve the highest physical stability could also be affected by moisture. Therefore, it is of importance to expand the investigations of co-amorphous systems towards storage under elevated, i.e., more humid conditions.

In this study, carvedilol (CAR) and L-aspartic acid (ASP) were chosen as the model drug and the co-former, respectively. The findings for co-amorphous CAR-ASP systems under dry storage conditions reported in our previous study can provide a comprehensive comparison with the results obtained under elevated storage conditions (Liu et al., 2020a). In CAR-ASP co-amorphous systems, salt formation was expected to occur between CAR and ASP at the 1:1 molar ratio based on their chemical structures. However, the optimal molar ratio to achieve the highest physical stability was found for the CAR-ASP 1:1.5 system under dry storage conditions (Liu et al., 2020a). Therefore, samples with different CAR to ASP molar ratios (3:1, 2:1, 1:1, 1:1.5, 1:2 and 1:3) were prepared by spray drying in the current study. After preparation, the samples were stored at two conditions, i.e., 25 °C 55%RH and 40 °C 55%RH. X-ray powder diffraction (XRPD), thermogravimetric analysis (TGA) and scanning electron microscopy (SEM) were performed to track physical stability, water content and morphology changes of the co-amorphous systems during storage. In order to obtain a deeper understanding of the systems' behavior, modulated differential scanning calorimetry (mDSC), Fourier-transformed infrared spectroscopy (FTIR) and

variable temperature XRPD (vtXRPD) measurements of samples before and after one week of storage under elevated conditions were also conducted.

2. Materials and methods

2.1. Materials

CAR (MW = 406.47 g/mol, polymorphic form II, Cambridge Structural Database Refcode GIVJUQ01) was obtained from Fagron Nordic AS (Copenhagen, Denmark). ASP (MW = 133.10 g/mol) and magnesium nitrate hexahydrate were purchased from Sigma-Aldrich (St. Louis, MO, USA). Ethanol was obtained from Merck KGaA (Darmstadt, Germany) (> 99.7%, HPLC grade). Water (18.2 M Ω) was freshly prepared using a MilliQ water system from ELGA LabWater (High Wycombe, UK).

2.2. Methods

2.2.1. Sample preparation

CAR-ASP co-amorphous samples were prepared by spray drying. A total of 1.25 g of CAR and ASP at varying molar ratios of CAR to ASP (3:1, 2:1, 1:1, 1:1.5, 1:2, 1:3) was dissolved in 250 mL 50% (v/v) ethanol-water mixtures. Subsequently, the solutions were spray dried using a mini spray dryer B-290 (Büchi Labortechnik AG, Flawil, Switzerland) equipped with an inert loop (Büchi B-295) and a dehumidifier (Büchi B-296). All samples were prepared under the following parameters: inlet temperature: 110 °C; outlet temperature: 42 \pm 2 °C (below the T_gs of all samples); atomizing air flow rate (at standard temperature and pressure): 667 L/h (40 mm on spray dryer); nitrogen drying gas flow: 40 m³/h (100% of aspirator rate); feed flow rate: 9 mL/min.

2.2.2. Standard XRPD and vtXRPD measurements

XRPD analysis were performed on an X'Pert PANalytical PRO X-ray diffractometer (PANalytical, Almelo, The Netherlands) equipped with a copper anode (Cu K α radiation, λ = 1.54187 Å). The

acceleration voltage and current were 45 kV and 40 mA, respectively. For standard XRPD measurements, the scans were taken from 5° to $30^{\circ} 2\theta$ in reflection mode, with a scan rate of $0.067^{\circ} 2\theta/s$ and a step size of $0.026^{\circ} 2\theta$. vtXRPD measurements were conducted using an Anton Paar CHC sample stage (Anton Paar GmbH, Graz, Austria) mounted to the diffractometer. vtXRPD measurements were performed at $25^{\circ}C$, and then in $10^{\circ}C$ intervals from 70 to $150^{\circ}C$, with a temperature increase rate of $5^{\circ}C/min$. Before each scan, an equilibrium step of 60 s was applied and subsequently samples were scanned between 5° and $30^{\circ} 2\theta$, with a scanning speed of $0.164^{\circ} 2\theta/s$ and a step size of $0.013^{\circ} 2\theta$. The data was collected and analyzed using the software packages X'Pert Data Collector and X'Pert Highscore Plus (PANalytical, Almelo, The Netherlands).

Furthermore, the experimentally obtained XRPD diffractograms were compared to the diffractograms of pure CAR and CAR hydrate deposited in the Cambridge Structural Database. The XRPD diffractograms of crystalline CAR form I, form II, form III, CAR hydrate form I and CAR hydrate form II were taken from the database with Refcodes GIVJUQ, GIVJUQ01, GIVJUQ02, UVOHET and UVOHET01, respectively.

2.2.3. Thermal analysis

Water content in the samples was assessed by TGA under a constant nitrogen flow rate of 50 mL/min. Approximately 10 mg of powder was placed in platinum pans and heated from room temperature to $200^{\circ}C$ at a heating rate of $10^{\circ}C/min$ in a Discovery TGA (TA Instruments, New Castle, USA). Weight loss (in percentage) was determined using Trios software (TA Instruments, New Castle, USA) and was taken as the water content. Each sample was measured in three independent measurements.

DSC measurements of the samples were performed using a Discovery DSC (TA Instruments, New Castle, USA) in the modulated temperature mode. Powder samples of approximately 2–6 mg were weighed in Tzero aluminium pans and closed with hermetically sealed lids. After an isothermal step of 5 min at $-20\text{ }^{\circ}\text{C}$, the samples were heated to $140\text{ }^{\circ}\text{C}$ at a heating rate of $2\text{ }^{\circ}\text{C}/\text{min}$ with an underlying modulation amplitude of $0.2120\text{ }^{\circ}\text{C}$ and a period of 40 s. A constant nitrogen flow rate of $50\text{ mL}/\text{min}$ was applied. The T_{gs} were determined from the midpoint of the step change of the reversing heat flow signal using Trios software (TA Instruments, New Castle, USA). Each sample was measured in three independent measurements.

Theoretical T_{gs} of the stored samples were calculated using the Gordon-Taylor equation and thereafter were compared with the experimental T_{gs} to assess possible molecular interactions. Due to the unknown interaction pattern in the three component systems, two approaches were used for the theoretical T_{gs} calculations: in the first approach the respective CAR-ASP co-amorphous system was taken as the first single “component” and water as the second component; in the other approach CAR, ASP and water were included as three individual components.

Using the first approach (i.e., regarding CAR-ASP co-amorphous system as the first single “component” and water as the second component), the theoretical T_{gs} of the stored CAR-ASP samples were predicted based on the Gordon-Taylor equation as shown below (Gordon and Taylor, 1952):

$$T_{\text{g}12} = \frac{w_1 \cdot T_{\text{g}1} + K \cdot w_2 \cdot T_{\text{g}2}}{w_1 + K \cdot w_2} \quad (1)$$

where $T_{\text{g}12}$ is the T_{g} (in K) of the stored CAR-ASP sample, $T_{\text{g}1}$, $T_{\text{g}2}$, w_1 , w_2 are the T_{gs} (in K) and the weight fractions of respective CAR-ASP system and the contained water. K is a constant and described by the following equation:

$$K = \frac{T_{\text{g}1} \cdot \rho_1}{T_{\text{g}2} \cdot \rho_2} \quad (2)$$

where ρ_1 and ρ_2 are the respective densities of the CAR-ASP system and water. The densities of CAR-ASP co-amorphous systems were approximated based on the following equation:

$$\rho_{\text{CAR-ASP co-amorphous system}} = w_{\text{CAR}} \cdot \rho_{\text{amorphous-CAR}} + w_{\text{ASP}} \cdot \rho_{\text{amorphous-ASP}} \quad (3)$$

where w_{CAR} and w_{ASP} are the weight fractions of CAR and ASP in the respective co-amorphous systems.

For the second approach (i.e., treating CAR, ASP and water as three individual components), an adjusted version of the Gordon-Taylor equation for ternary components was used to calculate the theoretical T_g s (Lu and Zografis, 1998):

$$T_{g123} = \frac{w_1 \cdot T_{g1} + K_1 \cdot w_2 \cdot T_{g2} + K_2 \cdot w_3 \cdot T_{g3}}{w_1 + K_1 \cdot w_2 + K_2 \cdot w_3} \quad (4)$$

where T_{g123} is the T_g (in K) of the stored CAR-ASP sample, T_{g1} , T_{g2} , T_{g3} , w_1 , w_2 , w_3 are the T_g s (in K) and the weight fractions of amorphous CAR, ASP and the contained water, respectively. K_1 and K_2 are constants and described by the following equations:

$$K_1 = \frac{T_{g1} \cdot \rho_1}{T_{g2} \cdot \rho_2} \text{ and } K_2 = \frac{T_{g1} \cdot \rho_1}{T_{g3} \cdot \rho_3} \quad (5)$$

where ρ_1 , ρ_2 and ρ_3 are the respective densities of amorphous CAR, ASP and water. The density and T_g of amorphous water are 1.000 g/cm³ and 135 K, respectively (Hancock and Zografis, 1994).

The density of amorphous CAR ($\rho_{\text{amorphous-CAR}}$) is 1.240 g/cm³ and the density of amorphous ASP ($\rho_{\text{amorphous-ASP}}$) is approximately 1.610 g/cm³ (Berlin and Pallansch, 1968; Liu et al., 2020a; Planinšek et al., 2011).

2.2.4. SEM measurements

The morphology of the samples was observed using a Hitachi TM3030 Tabletop SEM (Hitachi High-Technologies Corporation, Tokyo, Japan). The samples were sputter-coated with a gold layer

and subsequently mounted on an aluminum tab using a conductive carbon tape. Images were captured at an accelerating voltage of 15 kV with $2,000 \times$ magnification.

2.2.5. FTIR analysis

FTIR analysis was carried out using an MB3000 FTIR spectrometer (ABB Inc., Quebec, Canada) attached to an attenuated total reflectance accessory with a ZnSe crystal plate (MIRacle™ Single Reflection ATR, PIKE Technologies, Fitchburg, US). The spectra were collected over a wavenumber range from 4000 to 400 cm^{-1} (64 scans, resolution 4 cm^{-1}) using Horizon MB software (ABB Inc., Quebec, Canada).

2.2.6. Analysis of amorphous samples during storage under elevated conditions

Samples were analyzed at the day of preparation and then were stored in desiccators at $25\text{ }^{\circ}\text{C}$ 55%RH and at $40\text{ }^{\circ}\text{C}$ 55%RH for further analysis. Saturated magnesium nitrate solution was used to obtain the required humidity in the desiccators. Temperature and humidity were monitored using a temperature-humidity data logger LOG32 TH (Dostmann Electronic GmbH, Wertheim, Germany).

Amorphous samples were regularly analyzed by XRPD, TGA and SEM during storage to track physical stability, water content and morphology changes, respectively. In addition, mDSC, FTIR and vtXRPD measurements of samples stored for one week were conducted and the results were compared with freshly prepared samples.

3. Results and discussion

3.1. Physical stability of samples during storage

After spray drying, the various CAR-ASP binary samples were measured by XRPD and mDSC to confirm the successful amorphization and the formation of homogenous single-phase co-

amorphous systems (data not shown). The results were consistent with our previous study (Liu et al., 2020a).

Co-amorphous systems with different molar ratios were stored under two conditions, i.e., 25 °C 55%RH and 40 °C 55%RH conditions, to investigate the influence of moisture at room temperature and elevated temperature on the physical stability of the co-amorphous systems. In general, samples at all molar ratios were more stable under the 25 °C 55%RH storage condition compared with the 40 °C 55%RH condition (Table 1). However, CAR-ASP 1:1 (and not CAR-ASP 1:1.5) showed the highest physical stability under both storage conditions, remaining amorphous for at least 47 weeks. In contrast, recrystallization occurred in all other samples at some time point during storage (see Table 1). Under both storage conditions, CAR-ASP samples became more stable from the CAR to ASP molar ratios 3:1 to 1:1, and the highest physical stability was observed at CAR-ASP 1:1, followed by a decrease in stability for samples with a further increased ASP concentration. This indicates that the optimal molar ratio to achieve the highest physical stability for CAR-ASP co-amorphous samples under these storage conditions was at the CAR to ASP 1:1 molar ratio. In contrast, in our previous study the optimal ratio of CAR-ASP systems under dry conditions was found to be at the CAR to ASP molar ratio 1:1.5, as that sample showed the highest physical stability and the highest T_g after spray drying (Liu et al., 2020a). Therefore, it can be concluded that the optimal molar ratio to achieve the highest physical stability of co-amorphous systems varies based on the presence of moisture. Furthermore, the T_g measured right after preparation cannot be used to predict the physical stability of this co-amorphous system when subsequently stored under elevated conditions. In addition, moisture from the non-dry storage conditions resulted in a decrease in the physical stability of CAR-ASP co-amorphous systems compared with the respective samples stored under dry conditions, with CAR-ASP systems at

molar ratios 1:1, 1:1.5 and 1:2 all being stable for at least 7 months under 25 °C dry and 40 °C dry conditions (Liu et al., 2020b).

Interestingly, the recrystallized components from the stored samples were different for the two storage conditions. As shown in Table 1, pure amorphous CAR recrystallized into form II when stored at 25 °C 55%RH, while reflections of both form II and form III were observed by XRPD for the samples stored at 40 °C 55%RH. As CAR form III is more stable than form II (Prado et al., 2014), the crystallization behavior follows Ostwald's rule of stages, with the initial appearance of the metastable form II. At higher degrees of absolute water content in the environment (Engebretsen et al., 2016), the more stable form III can be observed already. For CAR-ASP samples with excess CAR, the recrystallization reflections corresponded to CAR form II when stored at 25 °C 55%RH, thereby behaving as similar to the pure CAR. On the other hand, the samples recrystallized into the CAR hydrate form when stored at 40 °C 55%RH. For the CAR-ASP systems with excess ASP, recrystallization reflections of ASP were seen for all mixtures under both storage conditions. Surprisingly when considering the optimal ratio under dry conditions, not only ASP but also CAR recrystallized from the CAR-ASP 1:1.5 sample under both storage conditions as well as for the CAR-ASP 1:2 sample stored at 40 °C 55%RH. This indicates the possibility of salt disproportionation occurring in CAR-ASP 1:2 and CAR-ASP 1:1.5 samples during storage under elevated conditions (Guerrieri and Taylor, 2009; Hsieh and Taylor, 2015). Furthermore, the presence of recrystallized ASP shifted the recrystallization of CAR from form II to form III.

3.2. Water content of samples during storage

The water content of the amorphous samples was tracked by TGA during the storage period (Figure 1). The various CAR-ASP spray dried samples showed a similar initial water content

(around 2%) which however, significantly increased within one week of storage. CAR-ASP co-amorphous samples with higher ASP concentration showed a higher increase in water content after one week of storage, except the already recrystallized CAR-ASP 1:3 at 40 °C 55%RH (corresponding to the XRPD result), which indicates that amorphous ASP was more hygroscopic compared with amorphous CAR. Within the water content tracking period, the water content of all CAR-ASP systems initially increased whereafter a stable level was maintained for a period of several weeks. Thereafter the water content declined upon (or after) recrystallization, as shown Figure 1a and 1b for the following samples: CAR-ASP 1:3 (25 °C 55%RH), CAR-ASP 1:2 (25 °C 55%RH and 40 °C 55%RH), CAR-ASP 1:1.5 (40 °C 55%RH). A corresponding loss of water was not observed if the CAR-ASP sample recrystallized into the hydrate form (as observed in CAR-ASP 3:1 at 40 °C 55%RH).

The highest water content before recrystallization of CAR-ASP systems with excess CAR was slightly higher at the 40 °C 55%RH storage condition compared to 25 °C 55%RH. In contrast, samples with excess ASP (except the already recrystallized CAR-ASP 1:3) showed higher water uptake at the 25 °C 55%RH storage condition rather than at 40 °C 55%RH. This indicates that excess CAR absorbed more water at 40 °C compared with 25 °C, whereas excess ASP absorbed more water at 25 °C even though the absolute water content in the air at 40 °C 55% RH is higher than at 25 °C 55%RH (Engebretsen et al., 2016). However, even though CAR-ASP systems with excess ASP absorbed less water at the 40 °C 55%RH storage condition, recrystallization occurred faster at 40 °C 55%RH compared to the 25 °C 55%RH storage condition. This indicates that recrystallization was influenced by both, absorbed water content and temperature.

3.3. Morphology changes of samples during storage

SEM images were taken to provide an indication about morphology changes of CAR-ASP co-amorphous samples during storage. All freshly prepared CAR-ASP co-amorphous samples showed similar spherical shapes, with a primary particle size of less than 15 μm . The small spherical particles initially appeared agglomerated to larger particles. Already after one day of storage, particles appeared fused together and over time became flake-like and eventually aggregated into one smooth large system (Figure 2, taking CAR-ASP 1:1.5 stored under 40 °C 55%RH condition as an example). Some white markings appeared on the surface when the samples started to recrystallize.

Morphological changes were thus obvious for the majority of co-amorphous samples within one week of storage, and a comparison of morphologies of various the CAR-ASP samples is shown in Figure 3. All freshly spray dried CAR-ASP samples showed similar initial spherical shapes. After storage at the 25 °C 55%RH storage condition for one week, no significant changes were observed for the CAR-ASP 2:1 and CAR-ASP 1:1 samples. However, obvious aggregations occurred at CAR-ASP samples with CAR to ASP molar ratios 3:1, 1:1.5, 1:2 and 1:3. In addition, CAR-ASP samples with a large excess of either CAR or ASP (compared with CAR-ASP 1:1) showed more obvious morphological changes after one week of storage at 25 °C 55%RH.

Samples stored at 40 °C 55%RH for one week showed significant morphology changes at all molar ratios compared to the freshly prepared samples. Despite bigger changes observed under 40 °C 55%RH compared to the samples under 25 °C 55%RH, similar morphology change tendencies were detectable for the samples at different molar ratios below and above CAR-ASP 1:1. CAR-ASP 1:1 was deformed to the lowest degree after one week of storage under both conditions, thus indicating a correlation with the physical stability.

3.4. Influence of one week of storage under elevated conditions on co-amorphous systems

3.4.1. Influence of one week of storage on the T_g s

Since T_g s commonly link to physical stability of co-amorphous systems (Dengale et al., 2016; Löbmann et al., 2013), T_g s of CAR-ASP co-amorphous samples were measured before and after one week of storage (Figure 4). For freshly prepared samples, the experimentally determined T_g s of the CAR-ASP systems initially increased with an increasing ASP concentration, reaching a maximum at the CAR-ASP 1:1.5 molar ratio, followed by a subsequent reduction in T_g s. The result was in agreement with our previous study (Liu et al., 2020a). In general, the T_g s of the stored CAR-ASP samples showed a gradual decrease with an increase of ASP concentration from CAR to ASP 2:1 to 1:3 under both storage conditions (except for the recrystallized CAR-ASP 1:3 sample stored at 40 °C 55%RH). Therefore, T_g s after storage cannot be used to predict physical stability of CAR-ASP as moisture in the stored samples had a plasticization effect (Van den Mooter et al., 2001). In order to further investigate the potential moisture influence on the molecular interactions between CAR and ASP, comparison of the experimental T_g s with the respective theoretical T_g s calculated from the Gordon-Taylor equation was conducted (Jensen et al., 2014). Due to the unknown interaction pattern in the three component systems, the theoretical T_g s were calculated using two approaches, one regarding the respective CAR-ASP co-amorphous system as the first single “component” and water as the second component, and the other one treating CAR, ASP and water as three individual components. The first approach yielded in a curve resembling somewhat the freshly prepared experimental T_g s, with a maximum T_g at around the 1:1.5 CAR to ASP molar ratio. In contrast, the second approach resulted in a more linear, declining correlation. The visual appearance of the T_g s of the stored samples, without an obvious maximum, indicates a disruption of the CAR-ASP salt formation responsible for the maximum and indicates that the calculation assuming three separate components more closely resembles reality. In detail, at the CAR to ASP

molar ratio 3:1, the experimental T_g s and the two theoretical T_g s of CAR-ASP system were quite close. In contrast, the experimental T_g s of CAR-ASP systems with molar ratios ranging from 2:1 to 1:3 were lower than the theoretical T_g s calculated regarding the CAR-ASP system as a single “component”, but higher than the theoretical T_g s when treating CAR, ASP and water as three individual components. This suggests that the original molecular interactions between CAR and ASP in CAR-ASP binary systems were partly disturbed by the absorbed moisture during storage.

3.4.2. Influence of one week of storage on the salt formation between CAR and ASP

FTIR measurements were performed on the CAR-ASP co-amorphous systems before and after one week of storage under elevated conditions to further explore the influence of moisture on the molecular interactions between CAR and ASP and the spectra for all ratios are shown in Figure 5a and 5b. Due to the high similarity between the FTIR spectra of freshly prepared and stored samples, spectral subtractions were used to clarify spectral differences. CAR and ASP were expected to interact with each other based on their chemical structures (Figure S1), and salt formation between CAR and ASP having been observed in a previous study (Liu et al., 2020a). The unbound $-\text{COOH}$ group from crystalline ASP showed a signal at the wavenumber range of $1650\text{--}1750\text{ cm}^{-1}$ (Barth, 2000), and this signal shifted to 1685 cm^{-1} to 1717 cm^{-1} after spray drying due to partial amorphization of the pure amino acid (Figure 5c). For the freshly prepared CAR-ASP co-amorphous systems, the unbound $-\text{COOH}$ group signal disappeared in the samples at CAR to ASP molar ratios of 3:1, 2:1 and 1:1, which indicates that salt formation occurred between CAR and ASP (Figure 5d). However, the signal of unbound $-\text{COOH}$ group re-appeared for these CAR-ASP systems after one week of storage at both $25\text{ }^\circ\text{C}$ 55%RH and $40\text{ }^\circ\text{C}$ 55%RH (Figure 5a and 5b). This suggests that moisture disturbed the molecular interactions between CAR and ASP, resulting in salt disproportionation. This is consistent with the findings obtained from the T_g comparison

study. Salt disproportionation has previously been reported in other solid state systems (Guerrieri and Taylor, 2009; Hsieh and Taylor, 2015; Stephenson et al., 2011), and moisture at high RH storage conditions has been used to promote the disproportionation process (Hsieh and Taylor, 2015).

3.4.3. vtXRPD measurements on the samples after one week of storage

vtXRPD measurements were conducted on the CAR-ASP samples after storage. A clear differentiation was observed based on the CAR-ASP ratio after one week of storage at 25 °C 55%RH (Figure 6). In the CAR-ASP 3:1 co-amorphous system crystalline CAR reflections appeared at 100 °C, followed by their disappearance at 120 °C due to melting behavior (Kissi et al., 2018); Crystalline ASP reflections were subsequently observed at 140 °C. Co-amorphous CAR-ASP samples at 2:1, 1:1 and 1:1.5 molar ratios only showed recrystallized ASP reflections from 140 °C. CAR-ASP 1:2 and 1:3 (i.e., co-amorphous systems with increasing ASP concentration) showed lower ASP recrystallization temperatures, with 120 °C for CAR-ASP 1:2 and 90 °C for CAR-ASP 1:3, respectively. The results suggests that excess CAR existed in CAR-ASP 3:1 and excess ASP existed in CAR-ASP 1:2 and CAR-ASP 1:3 co-amorphous systems, with the CAR-ASP samples with a larger degree of excess components showing lower recrystallization temperatures.

In addition, the vtXRPD measurements were also performed on the samples after one week of storage under 25 °C dry condition for comparison (Figure S2). For these samples only CAR-ASP 3:1 and CAR-ASP 1:3 showed recrystallization of CAR and ASP respectively below 140 °C. This further confirmed that the absorbed moisture in CAR-ASP samples led to a faster recrystallization during storage under elevated conditions compared to dry conditions.

This finding were even more obvious for the samples after one week of storage at 40 °C 55%RH (Figure 7). In this case, both CAR-ASP 3:1 and CAR-ASP 2:1 showed crystalline CAR reflections below 120 °C, and ASP recrystallized below 140 °C from the CAR-ASP co-amorphous systems with molar ratios 1:1.5, 1:2 and 1:3. This indicates that CAR-ASP 1:1 was the most stable system at the 40 °C 55%RH storage condition, which is agreement with the physical stability tests. In addition, CAR-ASP 1:1 showed the highest recrystallization temperature, with the recrystallization temperatures of other stored CAR-ASP co-amorphous samples gradually decreasing with increasing concentration of excess CAR (from CAR-ASP 1:1 to 3:1) or excess ASP (from CAR-ASP 1:1 to 1:3), respectively. Taken together, the data suggests that excess CAR and excess ASP existing in the CAR-ASP binary systems results in a recrystallization at a lower temperature after storage compared with the CAR-ASP co-amorphous sample at the optimal molar ratio. vtXRPD measurements thus show potential to be used as a tool to determine the optimal molar ratio for the co-amorphous systems, especially for samples stored under elevated conditions in which T_g cannot always be an accurate predictor of physical stability due to the moisture influence.

4. Conclusion

In this study, CAR-ASP co-amorphous systems with different molar ratios were investigated upon storage under non-dry conditions. The optimal molar ratio to achieve the highest stability was found at the CAR to ASP molar ratio of 1:1, which was contradictory with a previous finding showing CAR-ASP 1:1.5 to be the most stable one under dry storage conditions. Moisture in elevated conditions disturbed the molecular interactions between CAR and ASP, and resulted in salt disproportionation in the co-amorphous systems. The recrystallized components from co-amorphous CAR-ASP were dependent on the different molar ratios and storage conditions. The morphology of co-amorphous systems obviously changed after one week of storage under elevated

conditions, which can be used to track the differences in storage stability of the CAR-ASP samples at different molar ratios. vtXRPD measurements of the CAR-ASP samples after one week of storage under elevated conditions suggested that excess CAR or excess ASP leads to a faster recrystallization at a lower temperature compared to the CAR-ASP co-amorphous sample at the optimal molar ratio (1:1).

In conclusion, this study showed that the optimal molar ratio to achieve the highest physical stability in co-amorphous systems can be different between samples stored under dry conditions and under elevated conditions. This highlights the necessity to consider the influence of moisture on co-amorphous systems during storage. Morphology changes tracked by SEM and vtXRPD measurements showed a potential to be used as practical methods to predict the optimal molar ratio of the co-amorphous systems stored under non-dry conditions at an early stage of storage.

Acknowledgement

Jingwen Liu acknowledges the China Scholarship Council (201806350247) for financial support.

References

- Andronis, V., Yoshioka, M., Zografi, G., 1997. Effects of sorbed water on the crystallization of indomethacin from the amorphous state. *J. Pharm. Sci.*, 86, 346-351. <https://doi.org/10.1021/js9602711>.
- Babu, N.J., Nangia, A., 2011. Solubility advantage of amorphous drugs and pharmaceutical cocrystals. *Cryst. Growth Des.*, 11, 2662-2679. <https://doi.org/10.1021/cg200492w>.
- Barth, A., 2000. The infrared absorption of amino acid side chains. *Prog. Biophys. Mol. Bio.*, 74, 141-173. [https://doi.org/10.1016/S0079-6107\(00\)00021-3](https://doi.org/10.1016/S0079-6107(00)00021-3).
- Berlin, E., Pallansch, M.J., 1968. Densities of several proteins and L-amino acids in the dry state. *J. Phys. Chem.*, 72, 1887-1889. <https://doi.org/10.1021/j100852a004>.

- Bikiaris, D.N., 2011. Solid dispersions, part I: recent evolutions and future opportunities in manufacturing methods for dissolution rate enhancement of poorly water-soluble drugs. *Expert Opin. Drug Deliv.*, 8, 1501-1519. <https://doi.org/10.1517/17425247.2011.618181>.
- Dengale, S.J., Grohganz, H., Rades, T., Löbmann, K., 2016. Recent advances in co-amorphous drug formulations. *Adv. Drug Deliv. Rev.*, 100, 116-125. <https://doi.org/10.1016/j.addr.2015.12.009>.
- Dengale, S.J., Ranjan, O.P., Hussien, S.S., Krishna, B.S., Musmade, P.B., Gautham Shenoy, G., Bhat, K., 2014. Preparation and characterization of co-amorphous ritonavir-indomethacin systems by solvent evaporation technique: improved dissolution behavior and physical stability without evidence of intermolecular interactions. *Eur. J. Pharm. Sci.*, 62, 57-64. <https://doi.org/10.1016/j.ejps.2014.05.015>.
- Engelbrechtsen, K.A., Johansen, J.D., Kezic, S., Linneberg, A., Thyssen, J.P., 2016. The effect of environmental humidity and temperature on skin barrier function and dermatitis. *J. Eur. Acad. Dermatol. Venereol.*, 30, 223-249. <https://doi.org/10.1111/jdv.13301>.
- Gordon, M., Taylor, J.S., 1952. Ideal copolymers and the second-order transitions of synthetic rubbers. I. Non-crystalline copolymers. *J. Appl. Chem.*, 2, 493-500. <https://doi.org/10.1002/jctb.5010020901>.
- Grohganz, H., Löbmann, K., Priemel, P., Jensen, K.T., Graeser, K., Strachan, C., Rades, T., 2013. Amorphous drugs and dosage forms. *J. Drug Deliv. Sci. Tec.*, 23, 403-408. [https://doi.org/10.1016/S1773-2247\(13\)50057-8](https://doi.org/10.1016/S1773-2247(13)50057-8).
- Guerrieri, P., Taylor, L.S., 2009. Role of salt and excipient properties on disproportionation in the solid-state. *Pharm. Res.*, 26, 2015-2026. <https://doi.org/10.1007/s11095-009-9918-y>.

Han, J., Wei, Y., Lu, Y., Wang, R., Zhang, J., Gao, Y., Qian, S., 2020. Co-amorphous systems for the delivery of poorly water-soluble drugs: recent advances and an update. *Expert Opin. Drug Deliv.*, 17, 1411-1435. <https://doi.org/10.1080/17425247.2020.1796631>.

Hancock, B.C., Zografi, G., 1994. The relationship between the glass transition temperature and the water content of amorphous pharmaceutical solids. *Pharm. Res.*, 11, 471-477. <https://doi.org/10.1023/A:1018941810744>.

Hancock, B.C., Zografi, G., 1997. Characteristics and significance of the amorphous state in pharmaceutical systems. *J. Pharm. Sci.*, 86, 1-12. <https://doi.org/10.1021/js9601896>.

Hsieh, Y.L., Taylor, L.S., 2015. Salt stability-effect of particle size, relative humidity, temperature and composition on salt to free base conversion. *Pharm. Res.*, 32, 549-561. <https://doi.org/10.1007/s11095-014-1484-2>.

Jensen, K., Löbmann, K., Rades, T., Grohgan, H., 2014. Improving co-amorphous drug formulations by the addition of the highly water soluble amino acid, proline. *Pharmaceutics*, 6, 416-435. <https://doi.org/10.3390/pharmaceutics6030416>.

Jensen, K.T., Larsen, F.H., Löbmann, K., Rades, T., Grohgan, H., 2016. Influence of variation in molar ratio on co-amorphous drug-amino acid systems. *Eur. J. Pharm. Biopharm.*, 107, 32-39. <https://doi.org/10.1016/j.ejpb.2016.06.020>.

Kawabata, Y., Wada, K., Nakatani, M., Yamada, S., Onoue, S., 2011. Formulation design for poorly water-soluble drugs based on biopharmaceutics classification system: basic approaches and practical applications. *Int. J. Pharm.*, 420, 1-10. <https://doi.org/10.1016/j.ijpharm.2011.08.032>.

Kissi, E.O., Kasten, G., Löbmann, K., Rades, T., Grohgan, H., 2018. The role of glass transition temperatures in coamorphous drug–amino acid formulations. *Mol. Pharmaceutics*, 15, 4247-4256. <https://doi.org/10.1021/acs.molpharmaceut.8b00650>.

- Korhonen, O., Pajula, K., Laitinen, R., 2017. Rational excipient selection for co-amorphous formulations. *Expert Opin. Drug Deliv.*, 14, 551-569. <https://doi.org/10.1080/17425247.2016.1198770>.
- Laitinen, R., Löbmann, K., Grohgan, H., Priemel, P., Strachan, C.J., Rades, T., 2017. Supersaturating drug delivery systems: The potential of co-amorphous drug formulations. *Int. J. Pharm.*, 532, 1-12. <https://doi.org/10.1016/j.ijpharm.2017.08.123>.
- Laitinen, R., Löbmann, K., Strachan, C.J., Grohgan, H., Rades, T., 2013. Emerging trends in the stabilization of amorphous drugs. *Int. J. Pharm.*, 453, 65-79. <https://doi.org/10.1016/j.ijpharm.2012.04.066>.
- Liu, J., Grohgan, H., Lobmann, K., Rades, T., Hempel, N.J., 2021. Co-amorphous drug formulations in numbers: Recent advances in co-amorphous drug formulations with focus on co-formability, molar ratio, preparation methods, physical stability, in vitro and in vivo performance, and new formulation strategies. *Pharmaceutics*, 13, 389. <https://doi.org/10.3390/pharmaceutics13030389>.
- Liu, J., Rades, T., Grohgan, H., 2020a. Determination of the optimal molar ratio in amino acid-based co-amorphous systems. *Mol. Pharmaceutics*, 17, 1335-1342. <https://doi.org/10.1021/acs.molpharmaceut.0c00042>.
- Liu, J., Grohgan, H., Rades, T., 2020b. Influence of polymer addition on the amorphization, dissolution and physical stability of co-amorphous systems. *Int. J. Pharm.*, 588, 119768. <https://doi.org/10.1016/j.ijpharm.2020.119768>.
- Löbmann, K., Laitinen, R., Strachan, C., Rades, T., Grohgan, H., 2013. Amino acids as co-amorphous stabilizers for poorly water-soluble drugs–Part 2: Molecular interactions. *Eur. J. Pharm. Biopharm.*, 85, 882-888. <https://doi.org/10.1016/j.ejpb.2013.03.026>.

- Löbmann, K., Strachan, C., Grohganz, H., Rades, T., Korhonen, O., Laitinen, R., 2012. Co-amorphous simvastatin and glipizide combinations show improved physical stability without evidence of intermolecular interactions. *Eur. J. Pharm. Biopharm.*, 81, 159-169. <https://doi.org/10.1016/j.ejpb.2012.02.004>.
- Lu, Q., Zografi, G., 1998. Phase behavior of binary and ternary amorphous mixtures containing indomethacin, citric acid, and PVP. *Pharm. Res.*, 15, 1202-1206. <https://doi.org/10.1023/A:1011983606606>.
- Planinšek, O., Kovačič, B., Vrečer, F., 2011. Carvedilol dissolution improvement by preparation of solid dispersions with porous silica. *Int. J. Pharm.*, 406, 41-48. <https://doi.org/10.1016/j.ijpharm.2010.12.035>.
- Prado, L.D., Rocha, H.V.A., Resende, J.A.L.C, Ferreira, G.B., de Figueiredo Teixeira, A.M.R., 2014. An insight into carvedilol solid forms: effect of supramolecular interactions on the dissolution profiles. *CrystEngComm*, 16, 3168-3179. <https://doi.org/10.1039/C3CE42403K>.
- Rumondor, A.C., Taylor, L.S., 2010. Effect of polymer hygroscopicity on the phase behavior of amorphous solid dispersions in the presence of moisture. *Mol. Pharmaceutics*, 7, 477-490. <https://doi.org/10.1021/mp9002283>.
- Savjani, K.T., Gajjar, A.K., Savjani, J.K., 2012. Drug solubility: importance and enhancement techniques. *ISRN Pharm.*, 2012, 195727. <https://doi.org/10.5402/2012/195727>.
- Stephenson, G.A., Aburub, A., Woods, T.A., 2011. Physical stability of salts of weak bases in the solid-state. *J. Pharm. Sci.*, 100, 1607-1617. <https://doi.org/10.1002/jps.22405>.
- Van den Mooter, G., Wuyts, M., Blaton, N., Busson, R., Grobet, P., Augustijns, P., Kinget, R., 2001. Physical stabilisation of amorphous ketoconazole in solid dispersions with

polyvinylpyrrolidone K25. Eur. J. Pharm. Sci., 12, 261-269. [https://doi.org/10.1016/S0928-0987\(00\)00173-1](https://doi.org/10.1016/S0928-0987(00)00173-1).

Journal Pre-proofs

Figure captions

Figure 1. Water contents of CAR-ASP systems during storage at 25 °C 55% RH (a) and 40 °C 55% RH (b) for 12 weeks.

Figure 2. SEM images showing the morphology changes of the CAR-ASP 1:1.5 co-amorphous system during storage at 40 °C 55%RH. White arrows indicate the markings appeared during recrystallization.

Figure 3. SEM images showing the morphology of CAR-ASP samples with different molar ratios before (a) and after one week of storage at 25 °C 55%RH (b) and at 40 °C 55%RH (c).

Figure 4. Comparison between the experimental T_g s and the theoretical T_g s calculated based on the Gordon-Taylor equation of samples after one week of storage at 25 °C 55%RH (a) and 40 °C 55%RH (b) storage conditions.

Figure 5. FTIR spectra of freshly prepared samples subtracted from the FTIR spectra of the respective one week stored CAR-ASP samples for (a) samples stored at 25 °C 55%RH and (b) samples stored at 40 °C 55%RH. (c) FTIR spectra of the starting materials. (d) FTIR spectra of the freshly prepared CAR-ASP samples.

Figure 6. vtXRPD measurements of CAR-ASP samples after one week of storage at 25°C 55%RH.

Figure 7. vtXRPD measurements of CAR-ASP samples after one week of storage at 40°C 55%RH.

Table 1. Physical stability of pure amorphous CAR and CAR-ASP co-amorphous systems

Samples	25 °C 55%RH storage condition		40 °C 55%RH storage condition	
	Stable period	Origin of reflection	Stable period	Origin of reflection
Pure CAR	1 week	CAR form II	1 week	CAR form II and form III
CAR-ASP 3:1	19 weeks	CAR form II	5 weeks	CAR hydrate
CAR-ASP 2:1	25 weeks	CAR form II	17 weeks	CAR hydrate
CAR-ASP 1:1	Still stable after 47 weeks		Still stable after 47 weeks	
CAR-ASP 1:1.5	45 weeks	CAR form III and ASP	10 weeks	CAR form III and ASP
CAR-ASP 1:2	5 weeks	ASP	4 weeks	CAR form III and ASP
CAR-ASP 1:3	2 weeks	ASP	1 week	ASP

Co-amorphous systems:

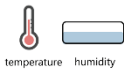
- Carvedilol-L-aspartic acid (CAR-ASP)

(CAR to ASP molar ratios ranging from 3:1 to 1:3)

↓ **Storage**

Non-dry conditions at two temperatures:

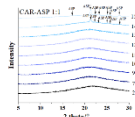
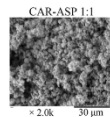
- 25 °C, 55%RH
- 40 °C, 55%RH

**The system with the highest physical stability**

- CAR-ASP 1:1 (molar ratio)
- Different from the one found at dry conditions

Influence of moisture on the molecular interactions**New options to predict the most stable system**

- Morphology changes tracked by SEM
- Variable temperature XRPD measurements



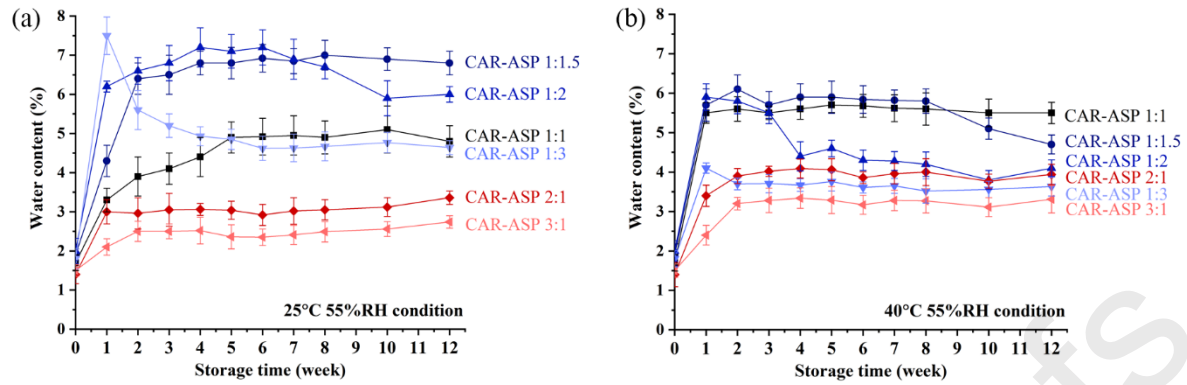
Journal Pre-proofs

Declaration of interests

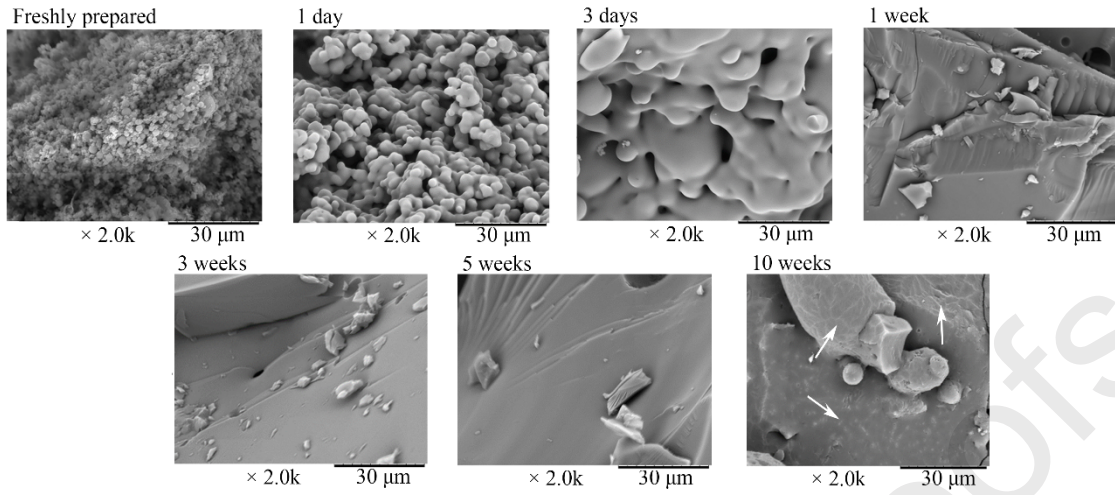
The authors declare that they have no known competing financial interests or personal relationships that could have appeared to influence the work reported in this paper.

The authors declare the following financial interests/personal relationships which may be considered as potential competing interests:

Journal Pre-proofs

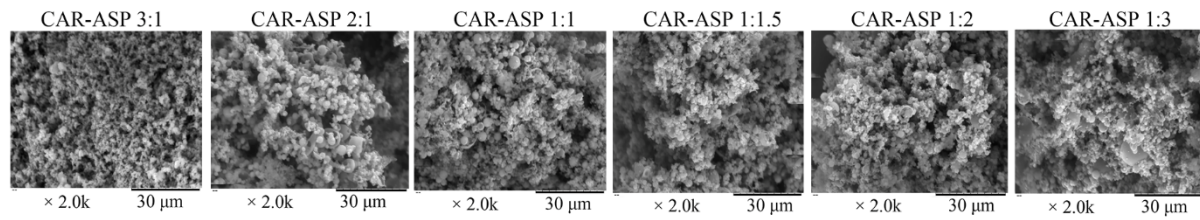


Journal Pre-proofs

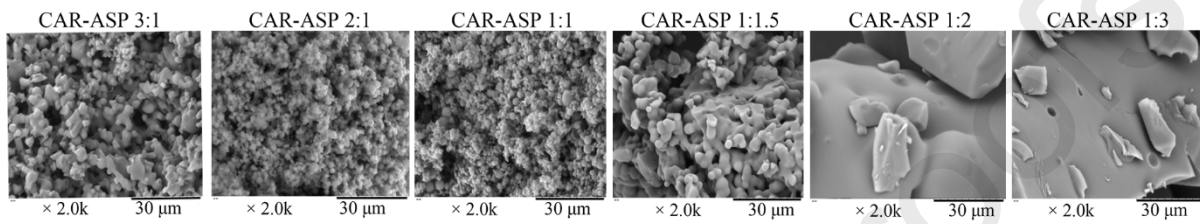


Journal Pre-proofs

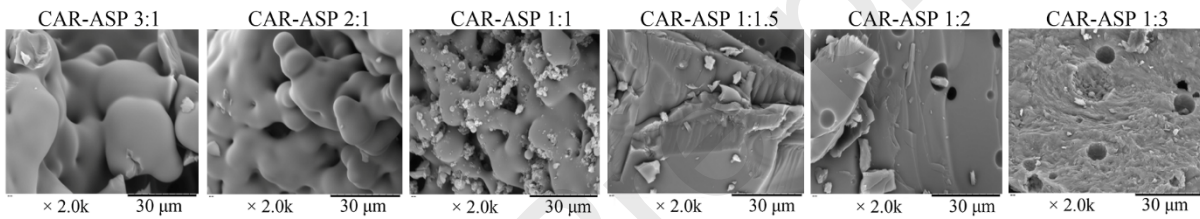
(a) Freshly prepared samples

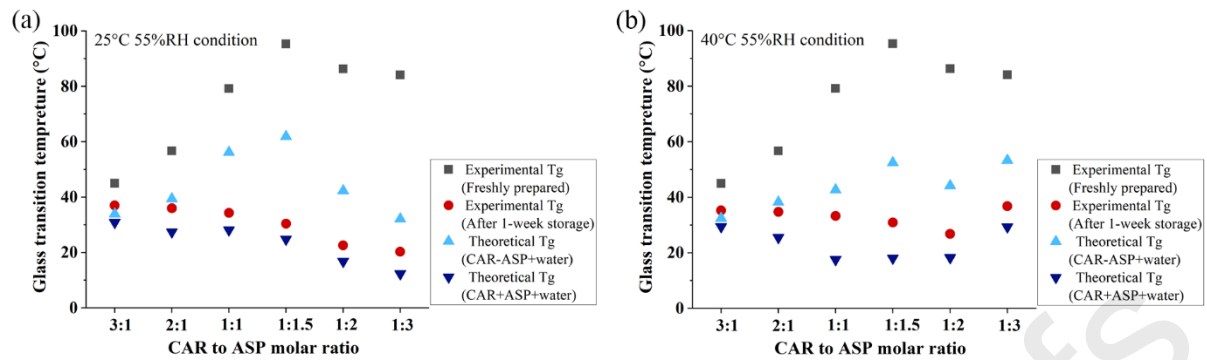


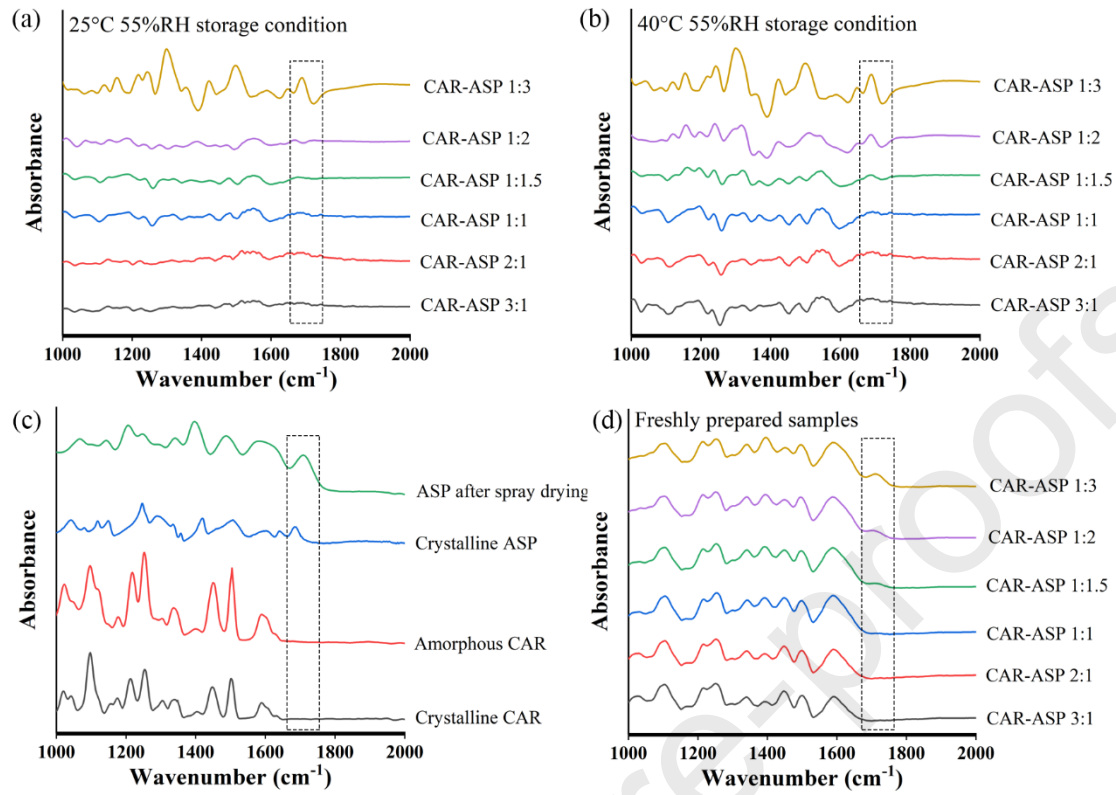
(b) After 1-week storage under 25°C 55%RH condition



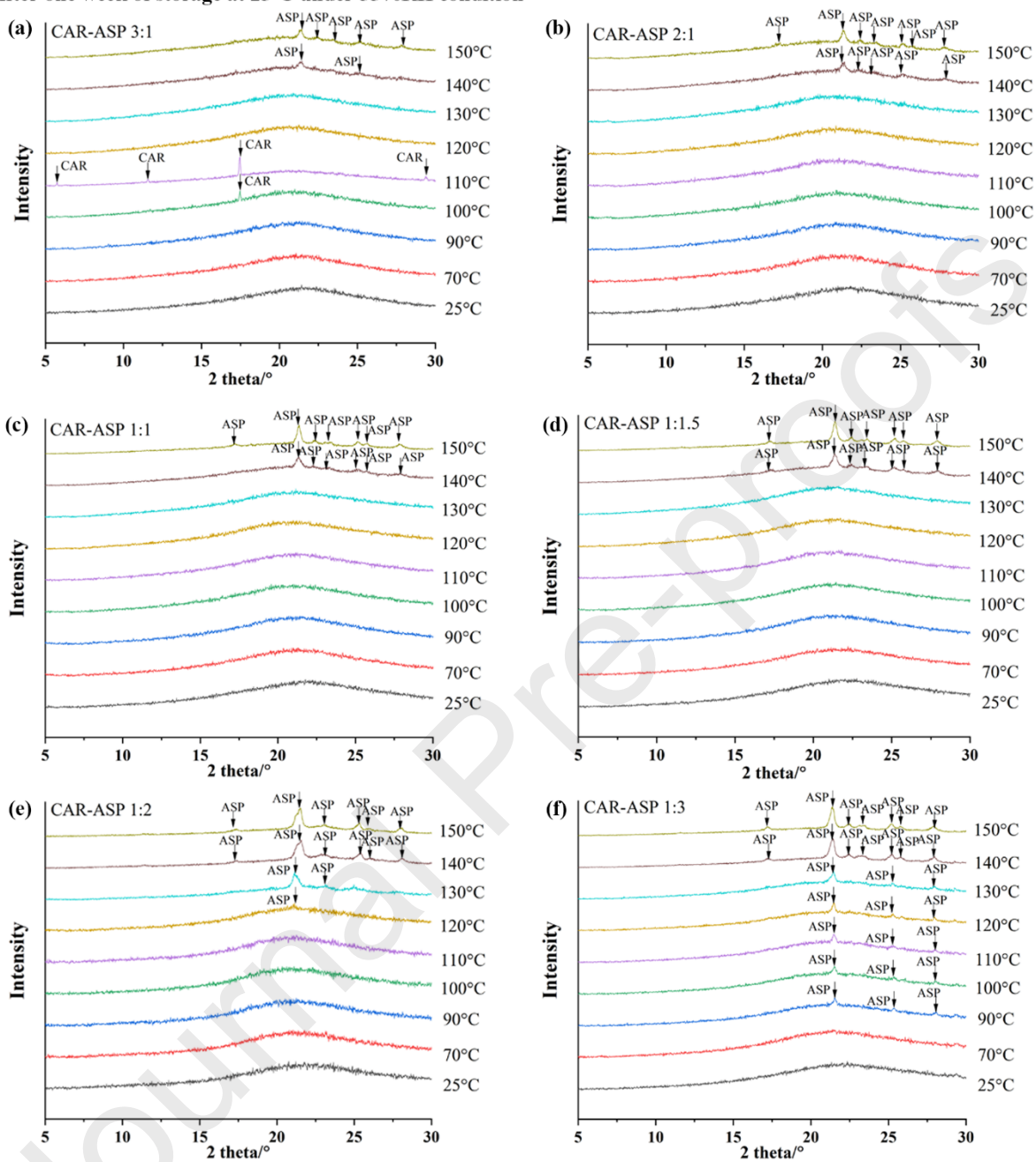
(c) After 1-week storage under 40°C 55%RH condition







After one week of storage at 25°C under 55%RH condition



After one week of storage at 40°C under 55%RH condition

